HHS Public Access

Author manuscript

Neuroscience. Author manuscript; available in PMC 2019 November 10.

Published in final edited form as:

Neuroscience. 2018 November 10; 392: 172–179. doi:10.1016/j.neuroscience.2018.09.035.

Striatal signaling regulated by the H3R histamine receptor in a mouse model of tic pathophysiology

Maximiliano Rapanelli, Ph.D.[1,†], **Luciana Frick, Ph.D.**[1,†], **Kantiya Jindachomthong, BS**[1], **Jian Xu, Ph.D.**[1,4], **Hiroshi Ohtsu, MD, Ph.D.**[2], **Angus Nairn, Ph.D.**[1,5], and **Christopher Pittenger, MD, Ph.D.**[1,3,4,5,*]

[1]Department of Psychiatry, Yale University

[2]Graduate School of Engineering, Tohoku University, Sendai, Japan

[3]Department of Psychology, Yale University

[4]Child Study Center, Yale University

[5]Interdepartental Neuroscience Program, Yale University

Abstract

Histamine dysregulation has been identified as a rare genetic cause of tic disorders; mice with a knockout of the *histidine decarboxylase* (*Hdc*) gene represent a promising model of this pathophysiology. How alterations in the histamine system lead to neuropsychiatric disease, however, remains unclear. The H3R histamine receptor is elevated in the striatum of *Hdc* KO mice, and H3R agonists, acting in the dorsal striatum, trigger tic-like movements in the model. In wild-type mice, H3R in the dorsal striatum differentially regulates MAPK and Akt signaling in D1R dopamine receptor-expressing striatonigral medium spiny neurons (dMSNs) and D2R dopamine receptor-expressing striatopallidal MSNs (iMSNs). Here we examined the effects of H3R agonist treatment on MSN signaling in the *Hdc*-KO model. In dMSNs, MAPK signaling was elevated at baseline in the *Hdc*-KO model, resembling what is seen after H3R activation in WT animals. Similarly, in iMSNs, Akt phosphorylation was reduced at baseline in the KO model, resembling what is seen after H3R activation in WT animals. H3R activation in *Hdc*-KO mice further enhanced the baseline effect on Akt phosphorylation in iMSNs but attenuated the abnormality in MAPK signaling in dMSNs. These observations support the hypothesis that constitutive activity of upregulated H3R receptors in the *Hdc*-KO model mediates the observed alterations in baseline MSN signaling; but further activation of H3R, which produces tic-like repetitive movements in the model, has more complex effects.

[*]Correspondence: Department of Psychiatry, Yale University, 34 Park Street, W315, New Haven, CT 06519, Christopher.pittenger@yale.edu 203-974-7675.
[†]Current address: University of Buffalo, Buffalo, NY

Conflicts of interests: none

Keywords

Tourette syndrome; Histidine decarboxylase; Histamine H3 receptor; dopamine receptor; medium spiny neurons; signaling pathway

INTRODUCTION

Tics are seen at least transiently in up to 20% of children, and a smaller fraction of adults. Tourette syndrome (TS), which consists of persistent vocal and motor tics, has a prevalence of ~0.7% (Scahill and Dalsgaard, 2013). Tics are commonly comorbid with other neuropsychiatric pathology, including obsessive-compulsive disorder (OCD), attentional difficulties, and autism (Martino and Leckman, 2013). Their etiology, however, remains poorly understood. Recently, dysregulation of histamine (HA) has been associated with TS, tic disorders, and related pathology (Pittenger, 2017). A rare mutation in the *histidine decarboxylase* (*Hdc*) gene, which is required for HA biosynthesis, was identified as a highpenetrance genetic cause of TS (Ercan-Sencicek et al., 2010; Castellan Baldan et al., 2014). *Hdc* knockout (KO) mice constitute a model of this pathophysiology (Pittenger, 2017). *Hdc* KO mice exhibit repetitive behavioral pathology (Castellan Baldan et al., 2014), including elevated grooming after acute stress (Xu et al., 2015). While such repetitive behaviors are not identical to tics, they suggest recapitulation of relevant pathological changes in the model. Other genetic studies have suggested that abnormalities in HA modulatory neurotransmission may contribute to tic disorders beyond the single pedigree in which the original *Hdc* mutation was identified (Fernandez et al., 2012; Karagiannidis et al., 2013).

Histamine acts on four G-protein-coupled receptors, H1R-H4R. The H3R receptor is expressed at high levels in the central nervous system (Haas et al., 2008; Panula and Nuutinen, 2013). It has high constitutive activity and can thus modulate intracellular signaling even in the absence of agonist (Morisset et al., 2000). H3R has classically been considered to be coupled to $G_{\alpha}i$ and to act presynaptically to reduce neurotransmitter release – both of HA itself and of other transmitters, including DA and glutamate (Schlicker et al., 1994; Haas et al., 2008; Ellender et al., 2011). More recently it has been found that much of the H3R in the striatum is post-synaptic, and that it couples to intracellular signaling cascades in striatal medium spiny neurons (MSNs) in complex and cell type-specific ways (Ferrada et al., 2008; Ferrada et al., 2009; Moreno et al., 2011; Panula and Nuutinen, 2013; Moreno et al., 2014; Rapanelli et al., 2016). H3R can heterodimerize with dopamine D1 and D2 receptors *ex vivo* and can modulate MAPK signaling (Ferrada et al., 2008; Ferrada et al., 2009; Moreno et al., 2011). We have replicated this regulation of MAPK signaling in D1-expressing striatonigral MSNs (dMSNs) *in vivo* (Rapanelli et al., 2016). In D2-expressing striatopallidal MSNs (iMSNs), in contrast, H3R activation modulates signaling through the Akt pathway (Rapanelli et al., 2016).

In a recent study we demonstrate that H3R is elevated in the striatum in *Hdc* KO mice, and its activation in the striatum produces stereotypies in this model (Rapanelli et al., 2017).

Here we characterize differential regulation of MAPK and Akt signaling in dMSNs and iMSNs by the H3R agonist R-aminomethyhistamine (RAMH) in *Hdc* KO mice.

EXPERIMENTAL PROCEDURES

Animals and treatment

All experiments were performed in accordance with the NIH Guide for the Use of Laboratory Animals and were approved by the Yale University Institutional Animal Care and Use Committee. Generation of *Hdc*-KO mice has been described previously (Ohtsu et al., 2001); our mice have been backcrossed onto C57BL/6J (Jackson Laboratory, Bar Harbor, ME, USA) for >10 generations and have been recently described (Castellan Baldan et al., 2014; Rapanelli et al., 2014; Xu et al., 2015). D1-DARPP-32-FLAG and D2-DARPP-32-Myc BAC transgenic mice have been previously described (Bateup et al., 2008) and were generously provided by Paul Greengard (Rockefeller University). *Hdc*-KO +/− mice were bred with D1-DARPP-32-FLAG/D2-DARPP-32-Myc double-homozygous mice for two generations to produce *Hdc*-KO $^{+/-}$ D1-DARPP-32-FLAG/D2-DARPP-32-Myc double-homozygous mice; these were intercrossed to produce *Hdc* KO and WT mice doubly transgenic for both D1-DARPP-32-FLAG and D2-DARPP-32-Myc, which were used for all experiments (hereinafter termed D1/D2-*Hdc*-KO or D1/D2-*Hdc*-WT mice). *Hdc* genotype was determined by PCR at weaning and confirmed after sacrifice.

Mice were housed in a temperature (23°) and humidity-controlled vivarium on a 12-h light/dark cycle. Two- to three-month old male and female mice were used in all experiments; sex was examined as an independent variable in all analyses but did not significantly affect any measured effects and thus is not reported.

R-(−)-α-Methylhistamine dihydrobromide (RAMH, Tocris Bioscience, Ellisville, MO, USA) was dissolved at 9 mg/ml in sterile saline. D1/D2-*Hdc*-KO and WT mice were injected with saline or RAMH (45 mg/kg, i.p.) for all experiments; this dose was motivated by previous studies (Rapanelli et al., 2017).

Immunohistochemistry

Thirty minutes after RAMH administration, D1/D2-*Hdc*-KO and WT mice were transcardially perfused with 4% paraformaldehyde in 1×PBS supplemented with 0.1 mM NaF. Brains were sliced on a cryostat at 30 μm; slices were stored in a solution containing 30% glycerin, 30% ethylene glycol, and 1×TBS plus 0.1 mM NaF. Slides were washed 3×10 min in TBS, incubated for 1 h at RT in TBS with 0.2% Triton X-100 and 5% donkey serum (Jackson Immunoresearch, West Grove, PA, USA), and then incubated overnight at RT in the same solution with goat anti-Myc antibody (Abcam, Cambridge, MA, USA; Cat# ab9132, 1:500), mouse anti-FLAG antibody (Sigma, St. Louis, MO, USA; Cat# F1804, 1:1000), and one of the following antibodies: rabbit anti-phospho-MSK1 Thr581 (Cell Signaling Technologies, Beverly, MA, USA; Cat# 9595P, 1:500), rabbit anti-phospho rpS6 S235/S236 (Cell Signaling Technologies; Cat #4858S, 1:500); rabbit anti-phospho rpS6 S240/S244 (Cell Signaling Technologies; Cat #5364P, 1:500); rabbit anti-phospho-Akt T308 (Cell Signaling Technologies; Cat #2965S 1:100). Slices were then rinsed 3×10 min at RT in

TBS with 0.2% Triton X-100 and 5% donkey serum, and then incubated for 1 h at RT in the same buffer with secondary antibodies: Alexa Fluor 555 donkey anti-rabbit (Life Technologies, Carlsbad, CA, USA; Cat# A31572, 1:500; excitation maximum 553 nm, emission maximum 568 nm), Alexa Fluor 633 donkey anti-goat (Life Technologies; Cat #A21082, 1:500; excitation maximum 621 nm, emission maximum 639 nm), and Alexa Fluor 488 donkey anti-mouse (Life Technologies; Cat# A21202, 1:500; excitation maximum 493 nm, emission maximum 519 nm). Slices were then rinsed in TBS, mounted on subbed slides, cover-slipped, and stored at 4°C.

Confocal imaging was performed by sequential scanning at 40× using an Olympus Fluoview FV-1000 confocal microscope equipped with 473 nm, 559 nm, and 635 nm lasers. Images were acquired with a Kalman filter at a scan rate of 4 μs/pixel. Twenty-μm Z-stacks were collected with a step size of 0.2 μm.

For each mouse, we collected serial coronal sections through the thickest portion of the dorsal striatum, from approximately bregma +1.0 mm to +0.15 mm (Paxinos and Franklin, 2004). Two nonadjacent sections were stained for each of the signaling phosphoproteins examined. Two confocal images were collected from each of these stained slides, one from the center of the dorsal striatum on each side, for a total of four images from each mouse for each staining condition. The images were collected centrally within the striatum such that they did not impinge on white matter of the internal capsule/corpus callosum or on adjacent structures, or on the anterior commissure/ventral striatum. Collecting a single central confocal image from the striatum on each side allowed maximum consistency of image placement across sections.

Cell counting was performed off-line, blind to experimental condition. All cell bodies that were positive for either FLAG (corresponding to D1R-expressing dMSNs) or Myc (corresponding to D2R-expressing iMSNs) were individually examined for immunostaining for signaling phosphoproteins. Cells in which phosphoprotein immunostaining above background colocalized in three dimensions with FLAG or Myc immunostaining were categorized as double-positive cells and counted. All FLAG- and Myc-positive cells in each captured image were thus categorized as either positive or negative for the stained phosphor-proteins. Data are expressed as double-positive cells as a percentage of all FLAG- or Myc-positive cells.

Statistical analysis

All values are expressed as mean ± SEM. Statistical analyses were performed using GraphPad Prism using two-way ANOVAs followed by Holm-Sidak's post-hoc test. Values were averaged from all images captured from each mouse before analysis; N therefore represents the number of animals, not the number of slices (2 from each mouse) or images (2 from each slice). All comparisons were considered significant at $P < 0.05$.

RESULTS

Hdc-KO mice show basal activation of the MAPK and AKT/GSK3β pathways in the dorsal striatum (Rapanelli et al., 2014). These signaling pathways are differentially regulated by the

H3 receptor in dMSNs and iMSNs in wild-type mice (Rapanelli et al., 2016). To better characterize their regulation with cell-type specificity in *Hdc*-KO mice, we crossed *Hdc*-KO mice with reporter mice in which dMSNs and iMSNs are labeled with distinct epitope tags (Bateup et al., 2008). We used triple-immunostaining for FLAG (the epitope tag that labels dMSNs), Myc (labeling iMSNs), and phospho-proteins implicated in MSN intracellular signaling, 30 min after saline or RAMH challenge.

Differential regulation of MSK phosphorylation by RAMH in dMSNs and iMSNs

We examined phosphorylation of MSK at T581, a MAPK target, in dMSNs and iMSNs.In dMSNs, there was a significant main effect of genotype (2×2 ANOVA: $F[1,28] = 6.3$, $p = 0.02$) and a genotype × treatment interaction ($F[1,28] = 45$, $P < 0.0001$), but no main effect of treatment (saline or RAMH: $F[1,28] = 0.005$, $P > 0.9$; **Figure 1**). *Post hoc* testing showed significant activation of MSK by RAMH in dMSNs, as we have previously reported (Rapanelli et al., 2016) (Holm-Sidak: $p < 0.001$). MAPK signaling was activated at baseline in *Hdc*-KO dMSNs (KO-saline vs WT-saline: $P < 0.0001$), in agreement with earlier findings that lacked cell-type specificity (Rapanelli et al., 2014). Unexpectedly, however, RAMH decreased MSK-T581 phosphorylation in *Hdc*-KO mice (KO-RAMH vs KO-saline: $P < 0.001$), suggesting a qualitative alteration in H3R signaling in dMSNs of *Hdc*-KO mice. RAMH-treated KO mice showed lower MSK phosphorylation than RAMH-treated WTs ($P < 0.05$).

MSK-T581 phosphorylation was not altered at baseline in iMSNs of *Hdc*-KO mice and was not regulated by RAMH challenge in iMSNs in either genotype (no significant main effects or interaction; **Figure 1**).

Differential regulation of ribosomal protein S6 phosphorylation by RAMH in dMSNs and iMSNs

Ribosomal protein S6 (rpS6) is phosphorylated at S235/S236 as a consequence of activation of the MAPK pathway, as well as several other signaling cascades (Meyuhas, 2008; Biever et al., 2015). We assayed rpS6 phosphorylation in dMSNs and iMSNs using triple-immunostaining. In dMSNs, there was a main effect of treatment ($F[1,28] = 14.8$, $p = 0.0006$) and a trend-level treatment x genotype interaction ($F[1,28] = 3.22$; $p = 0.08$); the main effect of genotype did not reach statistical significance ($F[1,28] = 2.37$; $p = 0.135$). RAMH treatment led to a significant increase in the phosphorylation of rpS6-S235/S236 in WT mice (Holm-Sidak: $p = 0.0026$), consistent with previous work (Rapanelli et al., 2016); there was no significant effect of RAMH in *Hdc*-KO mice (**Figure 2**).

In iMSNs, there were significant effects both of RAMH ($F[1,28] = 9.2$, $P = 0.005$) and genotype ($F[1,28] = 21.5$, $p < 0.0001$), but the interaction was not significant ($F[1,28] = 0.29$, $P = 0.6$). Phosphorylation of rpS6 in iMSNs after H3R activation was seen previously in wild-type mice, though it did not reach statistical significance in our previous study (Rapanelli et al, 2016, Figure 3B).

rpS6 phosphorylation at S235/236 was increased at baseline in *Hdc*-KO mice in both dMSNs and iMSNs. This parallels our previous demonstration of increased basal phosphorylation in these animals (Rapanelli et al, 2014).

We also examined phosphorylation of rpS6 at S240/S244, where phosphorylation is regulated by mTOR but not MAPK (Meyuhas, 2008; Biever et al., 2015). There were no significant changes of rpS6 phosphorylation at these sites in dMSNs at baseline or after RAMH challenge, although the main effect of genotype approached significance (genotype: $F[1,28] = 4.2$, $p = 0.051$; RAMH: $F[1,28] = 0.016$, $p > 0.9$; interaction: $F[1,28] = 0.77$, $p > 0.35$; **Figure 3**). In iMSNs, there was a significant main effect of genotype ($F[1,28] = 11.1$, $p < 0.0025$), but no effect of treatment ($F[1,28] = 2.1$, $P = 0.16$) or interaction ($F[1,28] = 1.5$, $P > 0.2$).

The nominal effects of genotype on rpS6 S240/S244 phosphorylation were in opposite directions in the two MSN types: basal phosphorylation was slightly reduced in dMSNs but slightly increased in iMSNs, compared to WT mice (**Figure 3**).

Differential regulation of Akt phosphorylation by RAMH in dMSNs and iMSNs

Finally, we examined phosphorylation of the signaling molecular Akt at T308, which we have previously shown to be regulated by H3R activation (Rapanelli et al., 2016) and in *Hdc*-KO mice (Rapanelli et al., 2014). There were no significant main effects or interactions in dMSNs. In iMSNs, on the other hand, there were highly significant main effects of both RAMH treatment and genotype, with no interaction (RAMH: $F[1,28] = 14.6$, $p = 0.0007$; genotype: $F[1,28] = 12.3$, $p = 0.0016$; interaction, $F[1,28] = 1.25$, $p = 0.27$; **Figure 4**). *Hdc* knockout reduced baseline Akt phosphorylation in iMSNs, explaining the reduced phosphorylation we have previously observed without dissociating cell types (Rapanelli et al., 2014). RAMH reduced T308 phosphorylation in iMSNs in both genotypes.

DISCUSSION

Alterations in the brain's histamine modulatory system have been implicated as a contributor to the development of tics and of TS by a series of genetic studies (Ercan-Sencicek et al., 2010; Fernandez et al., 2012; Karagiannidis et al., 2013). The *Hdc* knockout mouse recapitulates a rare but high-penetrance genetic cause of TS, inactivation of the *histidine decarboxylase* gene, and constitutes a promising model of tic pathophysiology (Ercan-Sencicek et al., 2010; Castellan Baldan et al., 2014; Pittenger, 2017). *Hdc*-KO mice exhibit repetitive behavioral pathology, DA dysregulation, altered histamine receptor levels, and elevated markers of cellular activity and intracellular signaling in the striatum (Dere et al., 2003; Castellan Baldan et al., 2014; Rapanelli et al., 2014; Xu et al., 2015).

H3R has historically been described as a presynaptic $G_{\alpha}i$-coupled receptor; it can negatively regulate the release of HA itself as well as of DA, glutamate, and other neurotransmitters (Schlicker et al., 1994; Haas et al., 2008; Ellender et al., 2011). However, it is increasingly clear that H3R also exists postsynaptically, in which context its signaling properties are complex and are modulated by its interactions with other cellular components, including DA receptors (Ferrada et al., 2008; Ferrada et al., 2009; Moreno et al., 2011; Moreno et al.,

2014). Indeed, postsynaptic signaling may be a primary function of the H3 receptor in the striatum (Panula and Nuutinen, 2013).

Distinct H3R signaling pathways in dMSNs and iMSNs have been described *ex vivo* (Ferrada et al., 2009; Moreno et al., 2011). We have recently replicated and extended this work *in vivo*, finding that H3R regulates MAPK signaling in dMSNs and Akt/GSK3β signaling in iMSNs in WT mice (Rapanelli et al., 2016). In the current study, we set out to determine whether MAPK and Akt signaling are also differentially regulated by H3R in *Hdc*-KO mice. We have previously shown this receptor to be upregulated in the striatum of these KO animals, both at the level of mRNA expression and at the level of radioligand binding (Rapanelli et al, 2017).

Several findings emerge. First, consistent with previous work (Ferrada et al., 2008; Ferrada et al., 2009; Moreno et al., 2011; Panula and Nuutinen, 2013; Moreno et al., 2014; Bolam and Ellender, 2015; Rapanelli et al., 2016), H3R signaling differentially affects intracellular signaling in dMSNs and iMSNs. This supports the conclusion that H3R interactions with other receptors, most prominently the D1R and D2R dopamine receptors, critically modulates its postsynaptic signaling properties. The one previously described effect of RAMH that we did not replicate here was the increased phosphorylation of Akt1 seen in dMSNs at an earlier time point (Rapanelli et al., 2016). This intriguing effect is transient – it is present 15 min after RAMH challenge but completely resolved by 45 min. It is likely that Akt regulation by RAMH in dMSNs is already resolved at the intermediate time point used in the current experiments (30 min after RAMH challenge).

Second, baseline signaling dysregulation in *Hdc*-KO MSNs differs in dMSNs and iMSNs.We have previously reported alterations in MAPK, rpS6, and Akt signaling in this knockout (Rapanelli et al., 2014). The current study adds nuance by dissociating effects in dMSNs and iMSNs. All abnormalities reported previously in undifferentiated striatum are replicated in the cell-specific effects here. Additionally, subtle alterations in rpS6 phosphorylation at S240/244 are seen in both cell types, but in opposite directions: basal phosphorylation of this site is reduced in *Hdc*-KO dMSNs and increased in iMSNs (only the latter effect reached statistical significance). This was not observed in undifferentiated striatum (Rapanelli et al., 2014), perhaps because the two effects obscure each other in when dMSNs and iMSNs are not examined separately. This emphasizes the utility of employing tools that allow separate quantification of signaling in the two MSN types.

Third, across all three signaling cascades examined, the baseline abnormalities seen in *Hdc*-KO mice resemble the effects seen after H3R activation in wild-type animals. Specifically, MAPK activity (indexed by MSK1 phosphorylation) is increased at baseline in dMSNs of *Hdc*-KO mice to a similar degree as it is after RAMH challenge in WT animals (**Figure 1**). Similar parallel effects are seen in both dMSNs and iMSNs in the regulation of P-S235/236 rpS6 (**Figure 2**), and in iMSNs in the dephosphorylation of Akt at T308 (**Figure 4**). H3R is constitutively upregulated in *Hdc*-KO mice (Rapanelli et al., 2014), presumably as a compensation for chronically deficient histamine. H3R has been shown in at least some contexts to have high basal activity, even in the absence of ligand (Morisset et al., 2000). This raises the intriguing possibility that many of the basal signaling abnormalities seen in

Hdc-KO mice are attributable to the baseline effects of elevated H3R expression, despite the absence of HA.

Fourth, H3R activation leads to augmentation of these signaling abnormalities, in most instances. In *Hdc*-KO mice, RAMH elevated phosphorylation of rpS6 in both dMSNs and iMSNs (though the effect was attenuated in dMSNs, possibly due to a ceiling effect) and further decreased phosphorylation of Akt in iMSNs. This accentuation of activity-dependent striatal signaling abnormalities may underlie the behavioral effects of RAMH documented previously in these mice (Rapanelli et al., 2017).

The exception to this pattern was in MAPK activity, as reflected in MSK phosphorylation at T581. MSK1 phosphorylation was elevated at baseline in dMSNs of *Hdc*-KO mice, but this elevation was attenuated by RAMH challenge; as a result there was a statistically significant interaction between genotype and drug condition in this analysis (**Figure 1B**). The cause of this interactive effect is unclear, but it suggests that H3R signaling may be qualitatively altered, not just amplified, in dMSNs. Alternatively, the activation of MAPK signaling by H3R activation may exhibit an inverted-U dose-response relationship, with phosphatases or other counterregulatory mechanisms being recruited only at higher levels of receptor activation. Further study is needed to elucidate these mechanistic details.

H3R activation reduces Akt phosphorylation in iMSNs in both genotypes (**Figure 4**), an effect similar to that produced by D2R activation in these cells via a β-arrestin-mediated mechanism (Beaulieu et al., 2004; Beaulieu et al., 2005; Beaulieu et al., 2011). Regulation of β-arrestin-mediated signaling by H3R has not been demonstrated to date, but it is possible that H3R regulates Akt via direct interaction with D2Rs, which has been described *ex vivo* (Ferrada et al., 2008);. Akt phosphorylation is reduced at baseline in iMSNs of the *Hdc*-KO mice. This may be because of constitutive activity of upregulated H3R; however, an alternative explanation is that tonically elevated DA in the *Hdc*-KO mouse striatum (Castellan Baldan et al., 2014; Rapanelli et al., 2014) provides sufficient D2R tone to reduce Akt phosphorylation via the D2-β-arrestin-Akt pathway, without the direct involvement of H3R.

Multiple signaling cascades converge on rpS6, including MAPK, S6 kinase, PKA, and mTOR (Meyuhas, 2008; Knight et al., 2012; Bonito-Oliva et al., 2013; Biever et al., 2015). We see alterations in rpS6 phosphorylation at S235/236 with both genotype and RAMH treatment, in both dMSNs and iMSNs. This site is regulated by the MAPK cascade; however, the dissociation between the effects seen on rpS6 and those seen on MSK1 suggest that other, convergent signaling pathways likely contribute. One possibility is the mTor pathway, although the lack of any modulation of the mTor-regulated S440/444 site on rpS6 argues against any central role for mTor. Another possibility is the PKA pathway; however, our previous work (Rapanelli et al, 2016) has revealed, perhaps surprisingly, that RAMH does not produce any detectable change in phosphorylation of DARPP-32, a major PKA target, *in vivo*. Further work is required to elucidate the complex interplay of different signaling pathways downstream of H3R in the striatum.

At baseline, *Hdc*-KO mice have alterations in the examined signaling cascades that resemble those seen in WT mice after RAMH challenge. Specifically, phosphorylation of MSK1 at T581 and of rpS6 ad S235/236 are elevated in dMSNs to a similar extent after saline in KO mice and after RAMH challenge in WT siblings. The same is true of the reduced phosphorylation of Akt at T308, specifically in iMSNs. A parsimonious explanation of this parallelism is that baseline signaling abnormalities in the KO animals derive from elevated basal H3R signaling. We have previously shown that H3R is upregulated in the *Hdc*-KO striatum (Rapanelli et al, 2017). In other contexts, .H3R has been shown to have a high degree of constitutive signaling activity, even in the absence of ligand (Morisset et al, 2000). If this high constitutive activity also occurs at postsynaptic H3Rs in the striatum (a possibility that has not yet been directly tested), then the upregulation of H3R seen in *Hdc*KO mice may lead to the observed baseline abnormalities in Msk1, rpS6, and Akt signaling, even in the absence of endogenous HA.

Other observations are not so easily explained by the upregulation of H3R in the *Hdc*KO striatum. Most strikingly, RAMH challenge decreases Msk1 phosphorylation in dMSNs, a qualitatively different effect from what is seen in WT animals. The mechanistic underpinnings of this qualitative alteration in signaling remain to be elucidated.

These molecular observations are best understood in the context of our previous behavioral work, in which we found RAMH challenge to produce stereotypies in the *Hdc*KO mouse (Rapanelli et al, 2017). Elevated stereotypic behavior is also seen in these animals after stress (Xu et al, 2016) or amphetamine challenge (Castellan Baldan et al, 2014), suggesting that they have a generalized instability of the striatal network that predisposes to repetitive behavioral pathology (Pittenger et al, 2017). The basline abnormalities in striatal signaling documented here may represent mechanistic correlates of this predisposition. This suggestion requires further investigation and, ideally, convergent support from other model systems.

This study has several limitations that must be addressed in future work. We have examined signaling *in vivo*; this has the advantage, relative to work in reduced systems, of preserving all connections and interactions in the intact brain, but it does not allow us to dissect mechanisms with the precision that is possible in *ex vivo* work. In addition, we have administered RAMH systemically, and thus we cannot rule out the possibility that peripheral drug effects contribute to the striatal phenomena documented here and in our previous work (Rapanelli et al, 2017). We counted cells from a limited number of sections per animal; this was necessary for all conditions to be evaluated in the same mice, but it may increase the variability of cell counts. We did not use stereological methods for cell counting, and our counts are thus relative, not absolute; this may also increase variability (Coggeshall and Lekan, 1996). These results require replication through convergent methods.

In summary, a disruption of the histaminergic signaling has been implicated in several neuropsychiatric disorders. Preclinical studies in the *Hdc*-KO mouse suggest that dysregulation of H3R can contribute to stereotypies, grooming, and other forms of repetitive behavioral pathology. *Hdc*-KO mice have been characterized as a model of tic pathophysiology (Pittenger, 2017). Our findings on the distinct intracellular signaling in

dMSNs and iMSNs in *Hdc*-KO mice may help clarify the mechanisms of H3R-induced repetitive behavioral pathology in the striatum.

Acknowledgements

This work was supported by The Allison Family Foundation (CP), the National Institute of Mental Health (R01MH091861, CP), a KAKENHI grant from JSPS (15H02358, HB), a Brain/MINDS program grant from AMED (HB), and the State of Connecticut through its support of the Ribicoff Research Facilities at the Connecticut Mental Health Center.

Abbreviations

Akt	protein kinase B
ANOVA	analysis of variance
cAMP	adenosine 3′,5′-cyclic monophosphate (cAMP)
DA	dopamine
dMSN	D1-expressing striatonigral MSN
GSK3β	Glycogen synthase kinase 3β
HA	histamine
HDC	histidine decarboxylase
iMSN	D2expressing striatonigral MSN
KO	knockout
MAPK	mitogen-activated protein kinase
MSK	mitogen- and stress-activated ki
MSNs	medium spiny neurons
mTOR	mammalian target of rapamycin
OCD	obsessive-compulsive disorder
RAMH	R-(−)-α-methylhistamine
rpS6	ribosomal protein S6
TS	Tourette syndrome
WT	wild typ

REFERENCES

Bateup HS, Svenningsson P, Kuroiwa M, Gong S, Nishi A, Heintz N, Greengard P (2008) Cell type-specific regulation of DARPP-32 phosphorylation by psychostimulant and antipsychotic drugs. Nat Neurosci 11:932–939. [PubMed: 18622401]

Beaulieu JM, Del'guidice T, Sotnikova TD, Lemasson M, Gainetdinov RR (2011) Beyond cAMP: The Regulation of Akt and GSK3 by Dopamine Receptors. Front Mol Neurosci 4:38. [PubMed: 22065948]

Beaulieu JM, Sotnikova TD, Marion S, Lefkowitz RJ, Gainetdinov RR, Caron MG (2005) An Akt/beta-arrestin 2/PP2A signaling complex mediates dopaminergic neurotransmission and behavior. Cell 122:261–273. [PubMed: 16051150]

Beaulieu JM, Sotnikova TD, Yao WD, Kockeritz L, Woodgett JR, Gainetdinov RR, Caron MG (2004) Lithium antagonizes dopamine-dependent behaviors mediated by an AKT/glycogen synthase kinase 3 signaling cascade. Proc Natl Acad Sci U S A 101:5099–5104. [PubMed: 15044694]

Biever A, Valjent E, Puighermanal E (2015) Ribosomal Protein S6 Phosphorylation in the Nervous System: From Regulation to Function. Front Mol Neurosci 8:75. [PubMed: 26733799]

Bolam JP, Ellender TJ (2015) Histamine and the striatum. Neuropharmacology.

Bonito-Oliva A, Pallottino S, Bertran-Gonzalez J, Girault JA, Valjent E, Fisone G (2013) Haloperidol promotes mTORC1-dependent phosphorylation of ribosomal protein S6 via dopamine- and cAMP-regulated phosphoprotein of 32 kDa and inhibition of protein phosphatase-1. Neuropharmacology 72:197–203. [PubMed: 23643747]

Castellan Baldan L et al. (2014) Histidine decarboxylase deficiency causes Tourette syndrome: parallel findings in humans and mice. Neuron 81:77–90. [PubMed: 24411733]

Coggeshall RE, Lekan HA (1996) Methods for determining numbers of cells and synapses: a case for more uniform standards of review. J Comp Neurol 364:6–15. [PubMed: 8789272]

Dere E, De Souza-Silva MA, Topic B, Spieler RE, Haas HL, Huston JP (2003) Histidine-decarboxylase knockout mice show deficient nonreinforced episodic object memory, improved negatively reinforced water-maze performance, and increased neo- and ventro-striatal dopamine turnover. Learn Mem 10:510–519. [PubMed: 14657262]

Ellender TJ, Huerta-Ocampo I, Deisseroth K, Capogna M, Bolam JP (2011) Differential modulation of excitatory and inhibitory striatal synaptic transmission by histamine. The Journal of neuroscience : the official journal of the Society for Neuroscience 31:15340–15351. [PubMed: 22031880]

Ercan-Sencicek AG et al. (2010) L-histidine decarboxylase and Tourette's syndrome. The New England journal of medicine 362:1901–1908. [PubMed: 20445167]

Fernandez TV et al. (2012) Rare copy number variants in tourette syndrome disrupt genes in histaminergic pathways and overlap with autism. Biological psychiatry 71:392–402. [PubMed: 22169095]

Ferrada C, Ferre S, Casado V, Cortes A, Justinova Z, Barnes C, Canela EI, Goldberg SR, Leurs R, Lluis C, Franco R (2008) Interactions between histamine H3 and dopamine D2 receptors and the implications for striatal function. Neuropharmacology 55:190–197. [PubMed: 18547596]

Ferrada C, Moreno E, Casado V, Bongers G, Cortes A, Mallol J, Canela EI, Leurs R, Ferre S, Lluis C, Franco R (2009) Marked changes in signal transduction upon heteromerization of dopamine D1 and histamine H3 receptors. British journal of pharmacology 157:64–75. [PubMed: 19413572]

Haas HL, Sergeeva OA, Selbach O (2008) Histamine in the nervous system. Physiol Rev 88:1183–1241. [PubMed: 18626069]

Karagiannidis I et al. (2013) Support of the histaminergic hypothesis in Tourette syndrome: association of the histamine decarboxylase gene in a large sample of families. Journal of medical genetics 50:760–764. [PubMed: 23825391]

Knight ZA, Tan K, Birsoy K, Schmidt S, Garrison JL, Wysocki RW, Emiliano A, Ekstrand MI, Friedman JM (2012) Molecular profiling of activated neurons by phosphorylated ribosome capture. Cell 151:1126–1137. [PubMed: 23178128]

Martino D, Leckman JF (2013) Tourette syndrome. Oxford; New York: Oxford University Press.

Meyuhas O (2008) Physiological roles of ribosomal protein S6: one of its kind. International review of cell and molecular biology 268:1–37. [PubMed: 18703402]

Moreno E, Hoffmann H, Gonzalez-Sepulveda M, Navarro G, Casado V, Cortes A, Mallol J, Vignes M, McCormick PJ, Canela EI, Lluis C, Moratalla R, Ferre S, Ortiz J, Franco R (2011) Dopamine D1-histamine H3 receptor heteromers provide a selective link to MAPK signaling in GABAergic neurons of the direct striatal pathway. The Journal of biological chemistry 286:5846–5854. [PubMed: 21173143]

Moreno E, Moreno-Delgado D, Navarro G, Hoffmann HM, Fuentes S, Rosell-Vilar S, Gasperini P, Rodriguez-Ruiz M, Medrano M, Mallol J, Cortes A, Casado V, Lluis C, Ferre S, Ortiz J, Canela E, McCormick PJ (2014) Cocaine disrupts histamine H3 receptor modulation of dopamine D1 receptor signaling: sigma1-D1-H3 receptor complexes as key targets for reducing cocaine's effects. The Journal of neuroscience : the official journal of the Society for Neuroscience 34:3545–3558. [PubMed: 24599455]

Morisset S, Rouleau A, Ligneau X, Gbahou F, Tardivel-Lacombe J, Stark H, Schunack W, Ganellin CR, Schwartz JC, Arrang JM (2000) High constitutive activity of native H3 receptors regulates histamine neurons in brain. Nature 408:860–864. [PubMed: 11130725]

Ohtsu H et al. (2001) Mice lacking histidine decarboxylase exhibit abnormal mast cells. FEBS Lett 502:53–56. [PubMed: 11478947]

Panula P, Nuutinen S (2013) The histaminergic network in the brain: basic organization and role in disease. Nature reviews Neuroscience 14:472–487. [PubMed: 23783198]

Paxinos G, Franklin KBJ (2004) The mouse brain in stereotaxic coordinates, Compact 2nd Edition. Amsterdam; Boston: Elsevier Academic Press.

Pittenger C (2017) Histidine Decarboxylase Knockout Mice as a Model of the Pathophysiology of Tourette Syndrome and Related Conditions. Handb Exp Pharmacol 241:189–215. [PubMed: 28233179]

Rapanelli M, Frick L, Pogorelov V, Ohtsu H, Bito H, Pittenger C (2017) Histamine H3R receptor activation in the dorsal striatum triggers stereotypies in a mouse model of tic disorders. Transl Psychiatry 7:e1013. [PubMed: 28117842]

Rapanelli M, Frick LR, Pogorelov V, Ota KT, Abbasi E, Ohtsu H, Pittenger C (2014) Dysregulated intracellular signaling in the striatum in a pathophysiologically grounded model of Tourette syndrome. European neuropsychopharmacology: the journal of the European College of Neuropsychopharmacology 24:1896–1906. [PubMed: 25464894]

Rapanelli M, Frick LR, Horn K, Schwarcz R, Pogorelov V, Nairn AC, Pittenger C (2016) The histamine H3 receptor differentially modulates MAPK and Akt signaling in striatonigral and striatopallidal neurons. The Journal of biological chemistry 291:21042–21052. [PubMed: 27510032]

Scahill L, Dalsgaard S (2013) Prevalence and methods for population screening In: Tourette Syndrome (Martno D, Leckman JF, eds). New York: Oxford University Press.

Schlicker E, Malinowska B, Kathmann M, Gothert M (1994) Modulation of neurotransmitter release via histamine H3 heteroreceptors. Fundam Clin Pharmacol 8:128–137. [PubMed: 8020871]

Xu M, Li L, Ohtsu H, Pittenger C (2015) Histidine decarboxylase knockout mice, a genetic model of Tourette syndrome, show enhanced stereotypy following stress. Neurosci Letters 595:50–53.

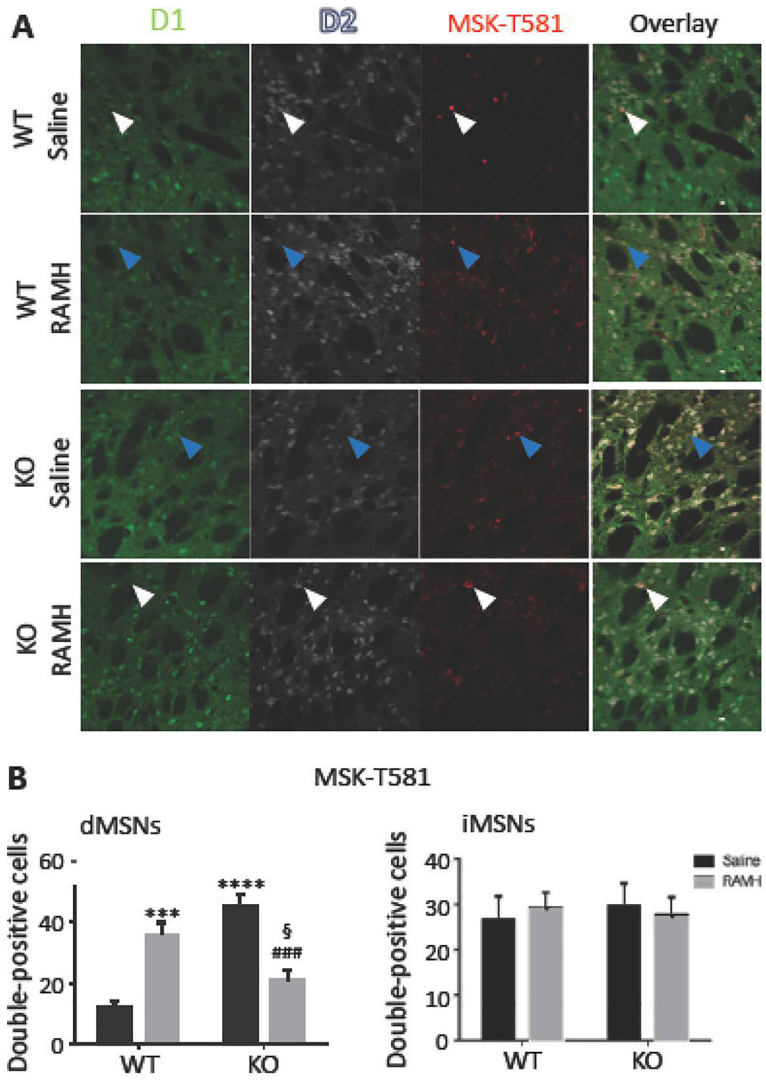

Fig. 1.

Regulation of MSK phosphorylation at T581 in D1-expressing striatonigral MSNs (dMSNs) after H3R activation. (A) D1/D2-*Hdc*-KO or D1/D2-*Hdc*-WT mice were injected with RAMH (45 mg/kg, i.p.) or saline and sacrificed 30 minutes post injection. Mouse brains were fixed and sliced on a cryostat at 30 μm. Brain slices were triple-immunolabeled using anti-FLAG (for D1-dMSNs), anti-Myc (for D2-iMSNs) and anti-phospho-T581 MSK antibodies. Representative images were shown. (B) MSK-T581 levels in dMSNs or iMSNs were quantitated on double-positive cells above background. Data were expressed as mean ± SEM. Statistical analyses were performed using two-ANOVO with post hoc Holm-Sidak multiple comparison test (*** $P < 0.001$, **** $P < 0.0001$ compared to WT-saline; ### $P < 0.001$ compared to KO-saline; § $P < 0.05$ compared to WT-RAMH; N = 8 per group). Here and throughout, white arrowheads indicate a sample phosphoprotein-positive iMSN; blue arrowheads indicate a sample positive dMSN. Scale bar, here and throughout, indicates 100 μm.

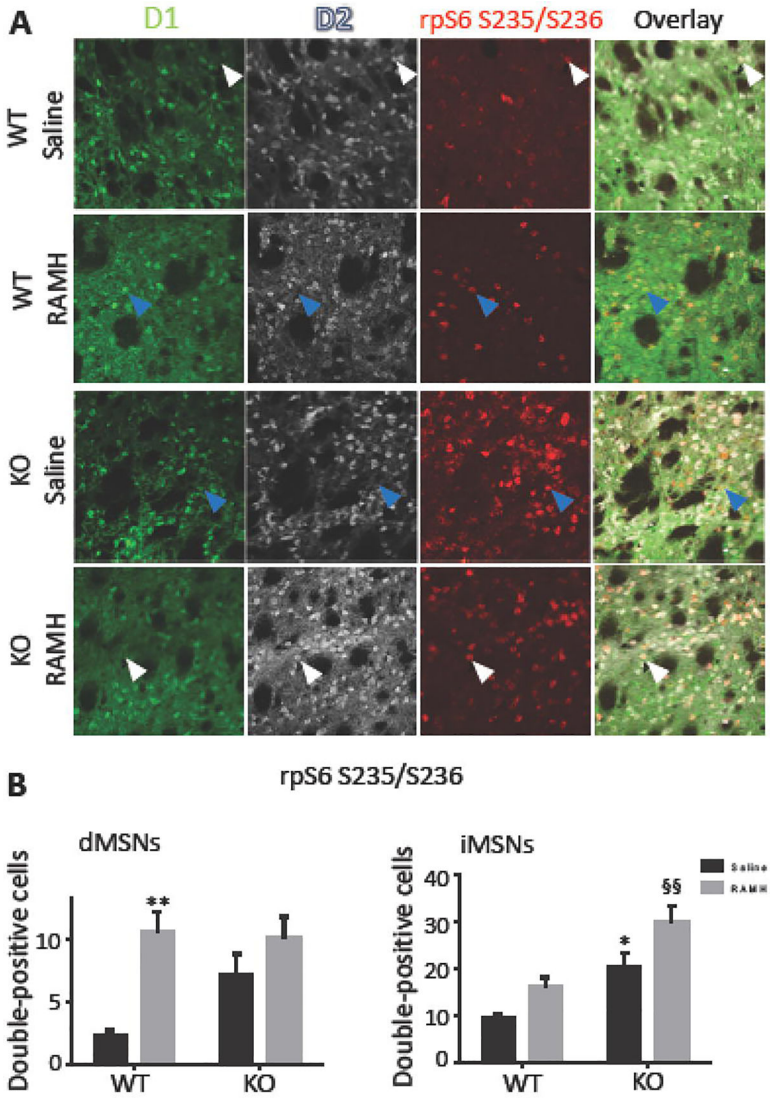

Fig. 2.

Regulation of rpS6 phosphorylation at S235/S236 in D1-expressing striatonigral MSNs (dMSNs) and D2-expressing striatopallidal MSNs (iMSNs) after H3R activation. (A) D1/D2-*Hdc*-KO or D1/D2-*Hdc*-WT mice were injected with RAMH (45 mg/kg, i.p.) or saline and sacrificed 30 minutes post injection. Mouse brains were fixed and sliced on a cryostat at 30 μm. Brain slices were triple-immunolabeled using anti-FLAG (for D1-dMSNs), anti-Myc (for D2-iMSNs) and anti-phospho- S235/S236 rpS6 antibodies. Representative images were shown. (B) rpS6-S235/S236 levels in dMSNs or iMSNs were quantitated on double-positive cells above background. Data were expressed as mean ± SEM. Statistical analyses were performed using two-ANOVO with post hoc Holm-Sidak multiple comparison test (* $P < 0.05$, ** $P < 0.01$ compared to WT-saline; §§ $P < 0.01$ compared to WT-RAMH; N = 8 per group).

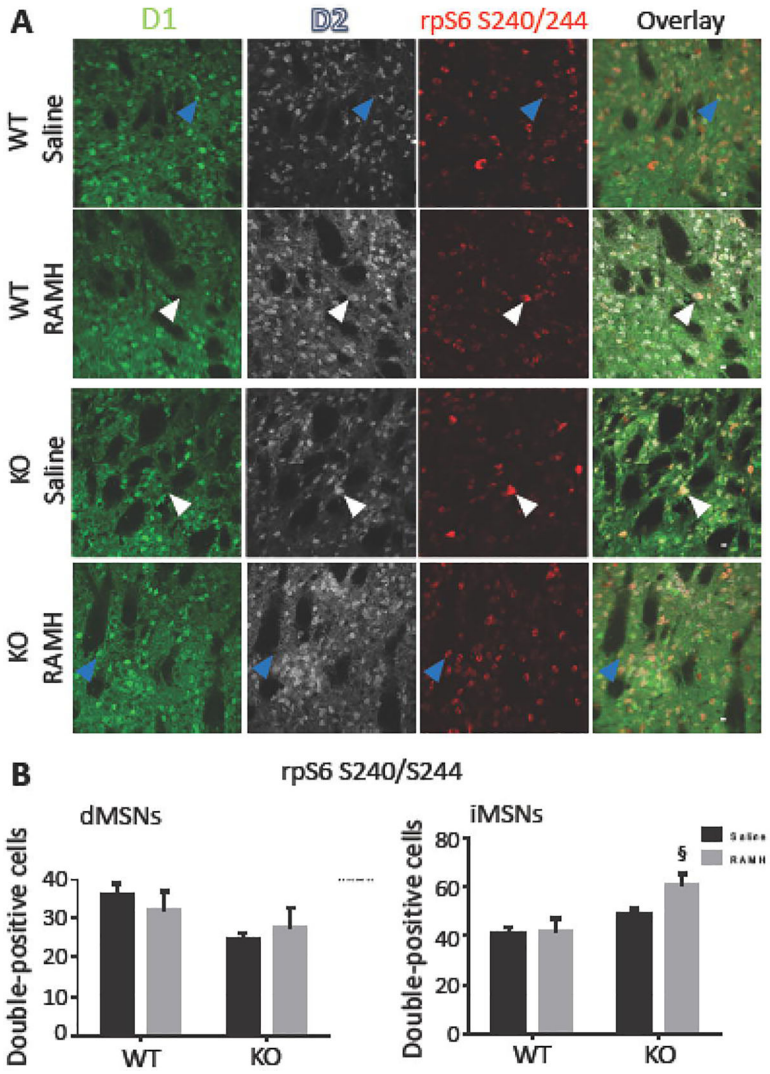

Fig. 3.

Regulation of rpS6 phosphorylation at S240/S244 in D2-expressing striatopallidal MSNs (iMSNs) after H3R activation. (A) D1/D2-*Hdc*-KO or D1/D2-*Hdc*-WT mice were injected with RAMH (45 mg/kg, i.p.) or saline and sacrificed 30 minutes post injection. Mouse brains were fixed and sliced on a cryostat at 30 μm. Brain slices were triple-immunolabeled using anti-FLAG (for D1-dMSNs), anti-Myc (for D2-iMSNs) and antiphospho-S240/S244 rpS6 antibodies. Representative images were shown. (B) rpS6S240/S244 levels in dMSNs or iMSNs were quantitated on double-positive cells above background. Data were expressed as mean ± SEM. Statistical analyses were performed using two-ANOVO with post hoc Holm-Sidak multiple comparison test (§ $P < 0.05$ compared to WT-RAMH; N = 8 per group).

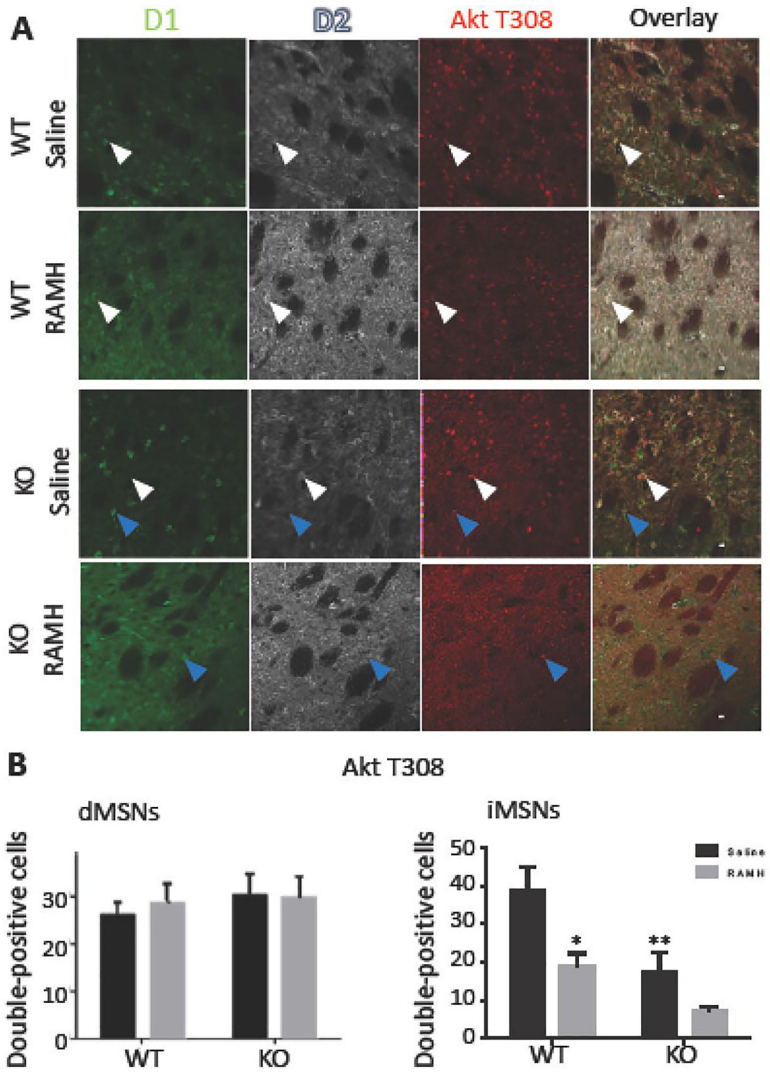

Fig. 4.

Regulation of Akt phosphorylation at T308 in D2-expressing striatopallidal MSNs (iMSNs) after H3R activation. (A) D1/D2-*Hdc*-KO or D1/D2-*Hdc*-WT mice were injected with RAMH (45 mg/kg, i.p.) or saline and sacrificed 30 minutes post injection. Mouse brains were fixed and sliced on a cryostat at 30 μm. Brain slices were triple-immunolabeled using anti-FLAG (for D1-dMSNs), anti-Myc (for D2-iMSNs) and anti-phospho-T308 Akt antibodies. Representative images were shown. (B) Akt-T308 levels in dMSNs or iMSNs were quantitated on double-positive cells above background. Data were expressed as mean ± SEM. Statistical analyses were performed using two-ANOVO with post hoc Holm-Sidak multiple comparison test (*$P < 0.05$, ** $P < 0.01$ compared to WT-saline; N = 8 per group).